

Low frequency spin dynamics in the quantum magnet copper pyrazine dinitrate

H. Kühne^{*1,2}, M. Günther¹, S.Grossjohann³, W. Brenig³, F.J. Litterst², A.P. Reyes⁴, P.L. Kuhns⁴, M.M. Turnbull⁵, C.P. Landee⁵, and H.-H. Klauss^{1,2}

¹ Institut für Festkörperphysik, TU Dresden, 01069 Dresden, Germany

² Institut für Physik der Kondensierten Materie, TU Braunschweig, 38106 Braunschweig, Germany

³ Institut für Theoretische Physik, TU Braunschweig, 38106 Braunschweig, Germany

⁴ National High Magnetic Field Laboratory, Tallahassee, Florida 32310, USA

⁵ Carlson School of Chemistry and Department of Physics, Clark University, Worcester, Massachusetts 01610, USA

PACS 64.70.Tg, 75.10.Jm, 75.30.Gw, 75.50.Ee

* Corresponding author: e-mail Kuehne@physik.tu-dresden.de, Phone: +49-351-46332404, Fax: +49-351-46337734

The $S=1/2$ antiferromagnetic Heisenberg chain exhibits a magnetic field driven quantum critical point. We study the low frequency spin dynamics in copper pyrazine dinitrate (CuPzN), a realization of this model system of quantum magnetism, by means of ^{13}C -NMR spectroscopy. Measurements of the nuclear spin-lattice relaxation rate T_1^{-1} in the vicinity of the saturation field are compared with quantum Monte Carlo calculations of the

dynamic structure factor. Both show a strong divergence of low energy excitations at temperatures in the quantum regime. The analysis of the anisotropic T_1^{-1} -rates and frequency shifts allows one to disentangle the contributions from transverse and longitudinal spin fluctuations for a selective study and to determine the transfer of delocalized spin moments from copper to the neighboring nitrogen atoms.

Copyright line will be provided by the publisher

1 Introduction Low dimensional quantum magnets, e.g. spin chains or ladders, are model systems for the study of quantum criticality [1,2,3,4,5,6,7,8,9]. For the isotropic $S=1/2$ antiferromagnetic Heisenberg chain (AFHC), nuclear magnetic resonance (NMR) has been used to probe the slow spin fluctuations in the full magnetic phase diagram of the AFHC, i.e., from the low to the high field limit and at temperatures from the quantum regime ($k_B T \ll J$) up to the classical regime ($k_B T \gg J$) [10]. The Hamiltonian of the AFHC in an external field reads:

$$H = \sum_i (J \mathbf{S}_i \cdot \mathbf{S}_{i+1} - g \mu_B \mathbf{B} \cdot \mathbf{S}_i), \quad (1)$$

where \mathbf{S}_i are spin operators and J is the exchange energy. At $B_c = 2J/(g\mu_B)$ the system exhibits a quantum critical phase transition, where a single Ising triplet as lowest elementary excitation crosses the ground state and the system switches from complete polarization into a Luttinger liquid of deconfined spinons. The condensation of low energy excitations is often referred to as critical slowing down and gives rise to a divergence of slow spin fluctuations.

In this paper we present a NMR study of the low frequency spin response for various magnetic fields close to $B_c = 14.9$ T [11] in the metalorganic AFHC copper pyrazine dinitrate (CuPzN). We discuss experimental data for fields from 2.0 to 14.8 T and temperatures from 1.6 to 30 K. The dynamics are probed by the nuclear spin-lattice relaxation rate T_1^{-1} and compared with quantum Monte Carlo (QMC) calculations. We also study the anisotropy of contributions from transverse and longitudinal spin fluctuations to T_1^{-1} and relate them to the anisotropic NMR frequency shift in the low field regime. The results are used to experimentally select the transverse spin fluctuations in the present work and to evaluate the spin density transfer from the copper ions to the neighboring nitrogen atoms in the pyrazine ring.

2 Experimental The compound CuPzN, i.e., $\text{Cu}(\text{C}_4\text{H}_4\text{N}_2)(\text{NO}_3)_2$ has been characterized by inelastic neutron scattering, muon-spin relaxation, magnetothermal transport, specific heat and magnetization measurements [11, 12, 13, 14]. All of these studies confirm CuPzN to be one of the best realizations of the AFHC with a low coupling

Copyright line will be provided by the publisher

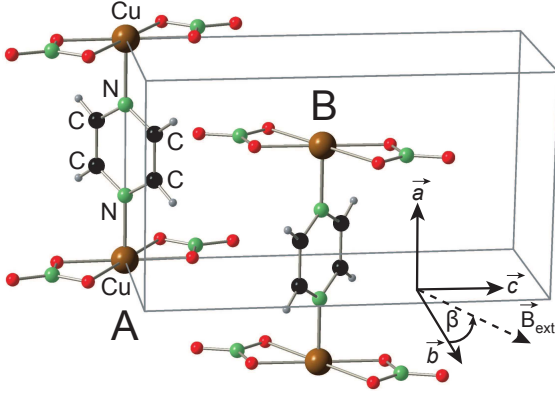


Figure 1 Segments of two neighboring chains A and B in the unit cell of CuPzN. The ^{13}C atoms reside in the pyrazine rings which are twisted against each other by $\simeq 80^\circ$ in the b - c plane.

constant $J/k_B = 10.7$ K. This low value of J allows the study of the magnetic QCP in standard laboratory magnets. The electronic $S = 1/2$ spins are mainly located in the Cu^{2+} 3d- orbitals, whereas the ^{13}C nuclei in the pyrazine ring were used as $I = 1/2$ NMR probes. The onsite copper nuclei exhibit an extremely short spin-correlation time that is below the dead time of a standard NMR spectrometer. The measurements were performed in an 8 and a 17 T superconducting magnet with a modified Bruker CXP200 spectrometer and a home-built spectrometer, respectively. In both cases a standard inversion-recovery spin-echo pulse sequence was used.

3 Nuclear Magnetic Resonance The nuclear spin-lattice relaxation rate T_1^{-1} measures the electronic spin fluctuations at the nuclear Larmor frequency ω_n . For the AFHC it can be written as [15]

$$\frac{1}{T_1} = \frac{\gamma_n^2}{2} \sum_q \sum_{\beta=x,y,z} [A_{x\beta}^2(q) + A_{y\beta}^2(q)] \times \int_{-\infty}^{\infty} \langle S_\beta(q, t) S_\beta(-q, 0) \rangle e^{-i\omega_n t} dt \quad (2)$$

$$= \frac{\gamma_n^2}{2} \sum_q [F_\perp(q) S_\perp(q, \omega_n) + F_z(q) S_z(q, \omega_n)]. \quad (3)$$

Here, $F_\perp(q) = \sum_{\beta=x,y} [A_{x\beta}^2(q) + A_{y\beta}^2(q)]$ and $F_z(q) = A_{xz}^2(q) + A_{yz}^2(q)$ are the geometrical form factors and $S_\perp(q, \omega)$ and $S_z(q, \omega)$ are the dynamical structure factors of the electronic spin system. $A_{\alpha\beta}$ with $\alpha, \beta = x, y, z$ are the components of the hyperfine coupling tensor $\underline{\mathbf{A}}(q)$.

3.1 Anisotropy of the NMR shift δ In CuPzN both an isotropic hyperfine part $\underline{\mathbf{A}}_{iso}(q)$ and an anisotropic dipolar part $\underline{\mathbf{A}}_{dip}(q)$ contribute to the coupling of the ^{13}C nuclei to the magnetic moments of the Cu^{2+} electrons. The NMR shift δ is proportional to the projection of the hyperfine coupling tensor $\underline{\mathbf{A}}(q = 0)$ on the direction of

the external field, i.e., the component $A_{zz}(0)$. Thus, for a rotation of the crystal in a fixed external field the shift can be extracted from:

$$\hat{\mathbf{A}}(0) = \underline{\mathbf{D}} \cdot ((\underline{\mathbf{A}}_{dip}(0) + \underline{\mathbf{A}}_{iso}(0)) \cdot \underline{\chi}_{el} + \underline{\sigma}) \cdot \underline{\mathbf{D}}^{-1}, \quad (4)$$

where $\underline{\chi}_{el}$ is the tensor of the electronic susceptibility, $\underline{\sigma}$ is the diamagnetic tensor, and $\underline{\mathbf{D}}$ is a rotation matrix. Fig. 2(a) shows the experimental shift $\delta(\beta)$ versus a simulation based on localized dipole moments for a rotation around the crystallographic a -axis, where $\beta = 0^\circ$ corresponds to an external field parallel to the b -axis, compare Fig. 1. The assumption that 100% of the spin magnetic moment resides on the Cu sites cannot describe the experimental data. A very good agreement is achieved for a spin moment transfer of 10% from copper to each of the neighboring nitrogen atoms in the pyrazine ring and a misalignment of 5° between the actual rotation axis and the crystallographic a -axis. The transfer of delocalized spin moments was observed in similar systems [16]. For the resulting isotropic hyperfine part we find $\delta_{iso} = 3600$ ppm. The existence of two sets of spectral lines results from the relative twisting of pyrazine rings on two neighboring chains by $\simeq 80^\circ$. According to Fig. 1, those will be labeled as line set A and B in the following.

3.2 Transverse dynamic structure factor Before turning to the T_1^{-1} data, we present our method of calculation for the field and temperature-dependent transverse dynamic structure factor $S_\perp(q, \omega_n)$. Switching to imaginary time τ the latter reads $S_\perp(q, \tau) = \frac{1}{\pi} \int_0^\infty d\omega S_\perp(q, \omega) K(\omega, \tau)$, with a kernel $K(\omega, \tau) = e^{-\tau\omega} + e^{-(\beta-\tau)\omega}$ and $\beta = 1/T$. In real-space $S_\perp(q, \tau)$ can be calculated efficiently, using QMC. Following Ref. [17]

$$S_{i,j}(\tau) = \left\langle \sum_{p,m=0}^n \frac{\tau^m (\beta - \tau)^{n-m} n!}{\beta^n (n+1)(n-m)! m!} \times S_i^+(p) S_j^-(p+m) \right\rangle_W, \quad (5)$$

where $S_\perp(q, \tau) = \sum_a e^{iqa} S_{a,0}(\tau)/N$ and $a, 0$ label lattice sites in a chain of length N . $\langle \dots \rangle_W$ refers to the Metropolis weight of an operator string of length n generated by the stochastic series expansion of the partition function [18, 19], and p, m are positions in this string.

Analytic continuation from imaginary times, i.e., $S_\perp(q, \tau)$, to real frequencies, i.e., $S_\perp(q, \omega)$, is performed by the maximum entropy method (MaxEnt), minimizing the functional $Q = \chi^2/2 - \alpha\sigma$ [20, 21]. Here χ refers to the covariance of the QMC data to the MaxEnt trial-spectrum $S_{\alpha\perp}(q, \omega)$. Overfitting is prevented by the entropy $\sigma = \sum_\omega S_{\alpha\perp}(q, \omega) \ln[S_{\alpha\perp}(q, \omega)/m(\omega)]$. We have used a flat default model $m(\omega)$, matching the zeroth moment of the trial spectrum. The optimal spectrum follows from the weighted average

$$S_\perp(q, \omega) = \int_\alpha d\alpha P[\alpha | S(q, \tau)] S_{\alpha\perp}(q, \omega), \quad (6)$$

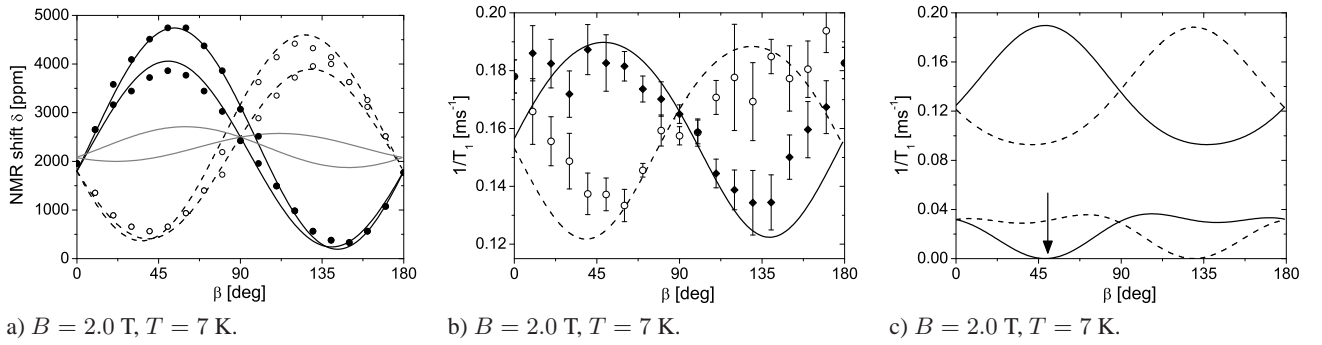


Figure 2 (a) NMR shift δ versus rotation angle β . As in (b) and (c), full (line set A) and dashed (line set B) lines correspond to calculations with a spin moment transfer of 10% in the simulation, gray lines correspond to a transfer of 0%. (b) Experimental T_1^{-1} -rates versus β compared with a modulation of T_1^{-1} based on Eqs. (3) and (4). (c) The modulation shown in (b) is disentangled into rates that stem from transverse (large values) and longitudinal (small values) fluctuations of the electronic moments. The arrow marks $\beta = 50^\circ$, where the latter rate of set A goes to zero.

with the probability distribution $P[\alpha|S(q, \tau)]$ adopted from Ref. [20].

3.3 Anisotropy of spin fluctuations The ratio of longitudinal and transverse spin fluctuations contributing to the total spin-lattice relaxation rate at a given field can be evaluated from the anisotropy of T_1^{-1} [22]. Our previous studies show that in this system the geometrical form factors for the case of ^{13}C -NMR are almost q -independent [10]. Therefore, the spin-lattice relaxation rate only depends on $S_\perp(q)$, $S_z(q)$ and the orientation between the external field and the local hyperfine fields, which in turn are well known from the study of $\delta(\beta)$. Fig. 2 (b) shows the experimental T_1^{-1} -rates versus a modulation of the relaxation rates based on equations (3), (4) and an almost isotropic dynamic structure factor calculated by QMC. The modulation was fitted to the experimental data by a single scaling factor determined by a least-squares fit. We find a good agreement for the comparison between our experimental data and the quantum Monte Carlo results. In this work we want to compare the experimentally and theoretically determined field- and temperature-dependent T_1^{-1} -rates stemming from transverse fluctuations only. Therefore, the contribution from longitudinal fluctuations $S_z(q, \omega)$ was minimized by minimizing $F_z(q)$. Fig. 2 (c) shows that for line set A the longitudinal fluctuation contribution to T_1^{-1} approaches zero for $\beta = 50^\circ$. This line set and orientation was used for the subsequent measurements shown in Figs. 3 and 4. Note that the transverse spin fluctuations also dominate the nuclear relaxation due to the large Fermi contact term in $F_\perp(q)$.

3.4 $1/T_1$: field dependence In Fig. 3 we compare the observed NMR rates with the QMC results versus magnetic field in the quantum regime $k_B T \ll J$, with $T = 1.6$ K. The QMC data shown in Figs. 3 and 4 were calculated from the transverse dynamic structure factor

$S_\perp(q, \omega)$ [23] and scaled with a factor assigned at 2.0 T and high temperatures. The similarity between experiment and theory is remarkable. For both we find a pronounced maximum of $T_1^{-1}(B)$ at $B = 13.8$ T shifting to lower fields with increasing temperature. To interpret these results, we note that in the fully polarized state for $B > B_c$, single magnons are exact eigenstates of Eq. (1) with a dispersion of

$$E_>(k) = J \cos(k) + g\mu_B B. \quad (7)$$

$E_>(k)$ displays a field-driven excitation gap of $g\mu_B B - J$ leading to an exponential decrease in $T_1^{-1}(B)$ at fixed T and for $B > B_c$. The rates calculated by QMC display a broader maximum than the measured data, but drop with the same slope for fields above 16 T. At $B = B_c$ the

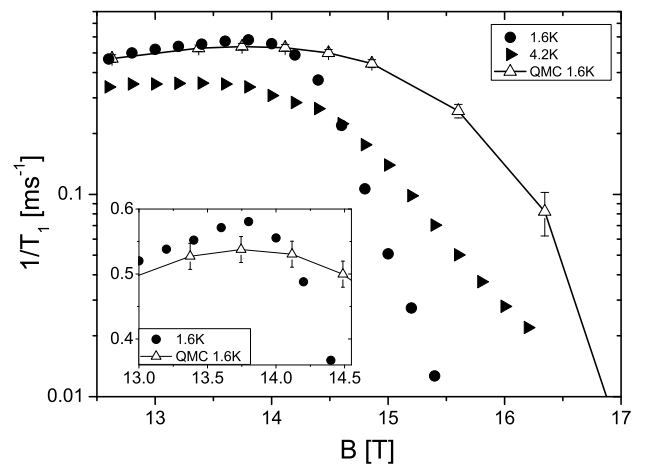


Figure 3 Field dependence of the nuclear spin-lattice relaxation rate of ^{13}C close to the critical field. The exponential decrease of data reflects the linear opening of the spin gap with field. The inset highlights the maximum of $T_1^{-1}(B)$ at $B = \tilde{B}_c$ and $T = 1.6$ K. All solid lines are a guide to the eye.

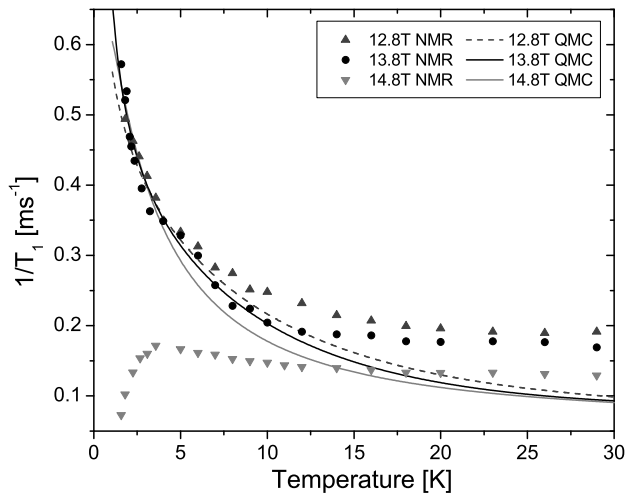


Figure 4 Temperature dependence of the nuclear spin-lattice relaxation rate of ^{13}C for different external fields in the vicinity of the quantum critical point. All QMC data lines are polynomial fits to analytic continuations of a 128 site system. The theoretical errors range from 10% at low temperatures to 20% at high temperatures, estimated from different MaxEnt regularization parameters.

dispersion touches the zero at $k = \pi/2$ with a *quadratic* momentum dependence yielding a van-Hove type of critical DOS. This leads to the maximum in T_1^{-1} , tending to diverge as $T \rightarrow 0$. For both, NMR experiment and QMC, the maximum in Fig. 3 occurs at $\tilde{B}_c \approx 13.8$ T, which is slightly less than the saturation field of $B_c = 14.9$ T for the magnetization. This downshift is most likely a finite-temperature effect of excitations populating the gap.

3.5 $1/T_1$: temperature dependence In Fig. 4 the temperature dependent T_1^{-1} rates for fields in the vicinity of the saturation field are shown. We find the strongest low temperature divergence at $\tilde{B}_c = 13.8$ T. This is very suggestive of critical scattering as $T \rightarrow 0$. With increasing temperature the van-Hove singularity in the DOS at B_c is smeared leading to the decrease in T_1^{-1} . At $B_c \simeq B = 14.8$ T the experimental data show no divergence but rather the opening of a spin gap. Possibly this field is slightly above the true saturation field for this orientation due to the sensitivity of the exact value of B_c to the anisotropic g -factor. The QMC data for 12.8 and 13.8 T show a satisfying agreement with the experiment, with the same divergence at low temperatures. In contrast to the experimental data, at 14.8 T there is still a divergence as the quantum regime is approached.

In the classical regime $k_B T \gg J$ the rate is decreasing with increasing fields. This is indicative of an excitation spectrum dominated by spin-diffusion modes from $q = 0$.

4 Conclusion We performed a complementary experimental and theoretical study of the low-frequency spin dynamics in the isotropic $S=1/2$ antiferromagnetic Heisen-

berg chain system copper pyrazine dinitrate. We find clear evidence for critical dynamics close to a field-induced QCP, as probed by the nuclear spin-lattice relaxation rate T_1^{-1} . Experimental data and QMC calculations are in good agreement and show a pronounced maximum in T_1^{-1} in the vicinity of the saturation field. In this study, the anisotropic contribution from longitudinal spin fluctuations to T_1^{-1} was minimized. From the analysis of the NMR frequency shift we conclude a spin moment transfer of 10% from copper to each of the neighboring nitrogen atoms in the pyrazine ring.

Acknowledgements Part of this work was performed at the National High Magnetic Field Laboratory, supported by NSF Cooperative under Agreement No. DMR-0084173, by the State of Florida, by the DOE and the DFG under Grants No. KL1086/6-2 and No. KL1086/8-1. One of us (W.B.) acknowledges partial support by the DFG through Grants No. BR 1084/4-1 and BR 1084/6-1. He also thanks the KITP for hospitality, where this research was supported in part by the NSF under Grant No. PHY05-51164.

References

- [1] B. C. Watson, V. N. Kotov, M. W. Meisel, D. W. Hall, G. E. Granroth, W. T. Montfrooij, S. E. Nagler, D. A. Jensen, R. Backov, M. A. Petruska, G. E. Fanucci, and D. R. Talham, *Phys. Rev. Lett.* **86**, 5168 (2001).
- [2] T. Lorenz, O. Heyer, M. Garst, F. Anfuso, A. Rosch, Ch. Rüegg, and K. Krämer, *Phys. Rev. Lett.* **100**, 067208 (2008).
- [3] Z. Honda, H. Asakawa, and K. Katsumata, *Phys. Rev. Lett.* **81**, 2566 (1998).
- [4] V. S. Zapf, D. Zocco, B. R. Hansen, M. Jaime, N. Harrison, C. D. Batista, M. Kenzelmann, C. Niedermayer, A. Lacerda, and A. Paduan-Filho, *Phys. Rev. Lett.* **96**, 077204 (2006)
- [5] S. A. Zvyagin, J. Wosnitza, C. D. Batista, M. Tsukamoto, N. Kawashima, J. Krzystek, V. S. Zapf, M. Jaime, N. F. Oliveira Jr., and A. Paduan-Filho, *Phys. Rev. Lett.* **98**, 047205 (2007)
- [6] H. Manaka, I. Yamada, Z. Honda, H. Aruga Katori, and K. Katsumata, *J. Phys. Soc. Jpn.* **67**, 3913 (1998).
- [7] V. O. Garlea, A. Zheludev, T. Masuda, H. Manaka, L.-P. Regnault, E. Ressouche, B. Grenier, J.-H. Chung, Y. Qiu, K. Habicht, K. Kiefer, and M. Boehm, *Phys. Rev. Lett.* **98**, 167202 (2007).
- [8] M. Takigawa, N. Motoyama, H. Eisaki, and S. Uchida, *Phys. Rev. Lett.* **76**, 4612 (1996).
- [9] G. Chaboussant, P. A. Crowell, L. P. Levy, O. Piovesana, A. Madouri, and D. Mailly, *Phys. Rev. B* **55**, 3046 (1997).
- [10] H. Kühne, H.-H. Klauss, S. Grossjohann, W. Brenig, F. J. Litterst, A. P. Reyes, P. L. Kuhns, M. M. Turnbull, and C. P. Landee, *Phys. Rev. B* **80**, 045110 (2009)
- [11] P. R. Hammar, M. B. Stone, D. H. Reich, C. Broholm, P. J. Gibson, M. M. Turnbull, C. P. Landee and M. Oshikawa, *Phys. Rev. B* **59**, 1008 (1999).
- [12] T. Lancaster, S. J. Blundell, M. L. Brooks, P. J. Baker, F. L. Pratt, J. L. Manson, C. P. Landee and C. Baines, *Phys. Rev. B* **73**, 020410(R) (2006).
- [13] M. B. Stone, D. H. Reich, C. Broholm, K. Lefmann, C. Rischel, C. P. Landee and M. M. Turnbull, *Phys. Rev. Lett.* **91**, 037205 (2003)

-
- [14] A. V. Sologubenko, K. Berggold, T. Lorenz, A. Rosch, E. Shimshoni, M. D. Phillips and M. M. Turnbull, *Phys. Rev. Lett.* **98**, 107201 (2007).
- [15] T. Moriya, *Prog. Theor. Phys.* **16**, 23 (1956).
- [16] A. U. B. Wolter, P. Wzietek, S. Söllow, F. J. Litterst, A. Honacker, W. Brenig, R. Feyerherm and H.-H. Klauss, *Phys. Rev. Lett.* **94**, 057204 (2005).
- [17] A. W. Sandvik, *J. Phys. A* **25**, 3667 (1992).
- [18] A. W. Sandvik, *Phys. Rev. B* **59**, R14157 (1999).
- [19] O. F. Syljuåsen and A. W. Sandvik, *Phys. Rev. E* **66**, 046701 (2002).
- [20] J. Skilling and R. K. Bryan, *Mon. Not. R. Astron. Soc.* **211**, 111 (1984).
- [21] M. Jarrell and J. E. Gubernatis, *Phys. Rep.* **269**, 133 (1996).
- [22] L. J. Azevedo, A. Narath, P. M. Richards and Z. G. Soos, *Phys. Rev. B* **21**, 2871 (1980).
- [23] S. Grossjohann and W. Brenig, *Phys. Rev. B* **79**, 094409 (2009)